1997

A Lagrangian dispersion model for predicting CO_2 sources, sinks, and fluxes in a uniform loblolly pine (*Pinus taeda* L.) stand

Gabriel Katul
Duke University

Ram Oren
Duke University

David Ellsworth
Duke University

Cheng-I Hsieh
Duke University

Nathan Phillips
Duke

See next page for additional authors

JOURNAL OF GEOPHYSICAL RESEARCH, VOL. 102, NO. D8, PAGES 9309–9321, APRIL 27, 1997

A Lagrangian dispersion model for predicting CO_2 sources, sinks, and fluxes in a uniform loblolly pine (*Pinus taeda L.*) stand

Gabriel Katul,[1] Ram Oren, David Ellsworth,[2] Cheng-I Hsieh, and Nathan Phillips
School of the Environment, Duke University, Durham, North Carolina

Keith Lewin
Department of Applied Sciences, Brookhaven National Laboratory, Upton, New York

Abstract. A canopy Lagrangian turbulent scalar transport model for predicting scalar fluxes, sources, and sinks within a forested canopy was tested using CO_2 concentration and flux measurements. The model formulation is based on the localized near-field theory (LNF) proposed by *Raupach* [1989a, b]. Using the measured mean CO_2 concentration profile, the vertical velocity variance profile, and the Lagrangian integral timescale profile within and above a forested canopy, the proposed model predicted the CO_2 flux and source (or sink) profiles. The model testing was carried out using eddy correlation measurements at 9 m in a uniform 13 m tall *Pinus taeda L.* (loblolly pine) stand at the Blackwood division of the Duke Forest near Durham, North Carolina. The tree height and spacing are relatively uniform throughout. The measured vertical profile leaf area index (LAI) was characterized by three peaks, with a maximum LAI occurring at 6.5 m, in qualitative agreement with the LNF source-sink predicted profile. The LNF CO_2 flux predictions were in better agreement with eddy correlation measurements (coefficient of determination $r^2 = 0.58$; and standard error of estimate equal to 0.16 mg kg^{-1} m s^{-1}) than K theory. The model reproduced the mean diurnal CO_2 flux, suggesting better performance over longer averaging time periods. Two key simplifications to the LNF formulation were considered, namely, the near-Gaussian approximation to the vertical velocity and the absence of longitudinal advection. It was found that both of these assumptions were violated throughout the day, but the resulting CO_2 flux error at 9 m was not strongly related to these approximations. In contrast to the forward LNF approach utilized by other studies, this investigation demonstrated that the inverse LNF approach is sensitive to near-field corrections.

1. Introduction

Quantifying the transfer of CO_2 and other scalar entities from leaves to the canopy scale continues to be a subject of active research [e.g., *Wofsy et al.*, 1993]. To properly quantify this transfer, detailed understanding of the canopy transport processes and the structure of turbulence within and above the canopy is required. The most comprehensive approach to quantify canopy scalar transport processes is to consider the scalar mass conservation equation given by

$$\frac{\partial C}{\partial t} + U_j \frac{\partial C}{\partial x_j} = k_c \frac{\partial^2 C}{\partial x_j \partial x_j} \tag{1}$$

where C is the instantaneous concentration of a scalar entity, k_c is the molecular diffusivity of the scalar C, U_j ($j = 1, 2, 3$) are the instantaneous velocity components ($U_1 = U$, $U_2 = V$, and $U_3 = W$), t is time, and x_j is the space coordinate system ($x_1 = x$, $x_2 = y$, $x_3 = z$), with x_1, x_2, and x_3 aligned along the longitudinal, lateral, and vertical directions, respectively. In this study, both meteorological and tensor notations are used interchangeably. The turbulent eddy motion inside the canopy is highly erratic and intermittent, so it is customary to apply Reynolds decomposition ($U_i = \langle U_i \rangle + u_i$; $C = \langle C \rangle + c$) to (1)

$$\frac{\partial \langle C \rangle}{\partial t} + \langle U_j \rangle \frac{\partial \langle C \rangle}{\partial x_j} = \frac{\partial}{\partial x_j}\left(k_c \frac{\partial \langle C \rangle}{\partial x_j} - \langle u_j c \rangle \right) \tag{2}$$

where angle brackets denote ensemble averaging assumed to converge to the time averaging by the ergodic hypothesis [*Monin and Yaglom*, 1971, pp. 215–218, 249–256] and $\langle u_i \rangle$ and $\langle c \rangle$ are both zero. Here, capital and lowercase letters represent instantaneous variables and turbulent fluctuations, respectively. Notice in (2) that both $\langle C \rangle$ and the covariance $\langle u_i c \rangle$ are unknown, and thus, (2) is not "closed."

As discussed by *Raupach* [1988], a popular closure approximation, known as K theory, assumes that the local relationship between the turbulent vertical flux of a scalar entity ($F_c = \langle wc \rangle$) and the mean concentration gradient is given by

$$F_c(z) = -K(z) \frac{d\langle C \rangle}{dz} \tag{3}$$

[1]Also at Center for Hydrologic Sciences, Duke University, Durham, North Carolina.
[2]Also at Department of Applied Sciences, Brookhaven National Laboratory, Upton, New York.

Paper number 96JD03785.
0148-0227/97/96JD-03785$09.00

where $K(z)$ is the eddy diffusivity. The K theory, or an Ohm's law resistance analog to K theory are widely used in climatic, hydrological, and ecological models such as the big-leaf model [e.g., *Van den Hurk and McNaughton*, 1995; *McNaughton and Van den Hurk*, 1995; *Dolman and Wallace*, 1991; *Meyers and Baldocchi*, 1988; *Dyer and Hicks*, 1970]. However, based on the detailed experiments of *Denmead and Bradley* [1985], it is recognized that K theory is inadequate for describing turbulent fluxes from local gradients within the canopy due to the strong variability in the sources and sinks of the scalar C, and due to the possible occurrence of countergradient transfer [also *Raupach*, 1988; *Wilson*, 1989; *Thurtell*, 1989]. Also, as noted by *Corrsin* [1974] and *Raupach* [1988], K theory is justifiable if the length scale of turbulent motion which maintains the turbulent flux F_c is much smaller than the length scale responsible for changes in the mean gradient $(d\langle C\rangle/dz)$. *Corrsin*'s [1974] condition for the application of K theory is violated in many canopy environments since the variability in sources and sinks of C introduces large variability in the profile of $\langle C\rangle$ within the canopy over short distances as evidenced by the data of *Raupach* [1988], *Wilson* [1989], and *Thurtell* [1989]. A suite of higher-order Eulerian closure models have been developed to circumvent some of the limitations of K theory [e.g., *Meyers and Paw U*, 1986, 1987; *Finnigan and Raupach*, 1987; *Meyers and Baldocchi*, 1988]. However, these models appear to be still flawed because gradient transfer schemes, analogous to K theory, are generally employed to attain closure for the higher-order statistics [e.g., *Deardorff*, 1978; *Sawford*, 1985; *Raupach*, 1988; *Baldocchi*, 1992].

Lagrangian models, which consider the mass conservation equation by following an infinitesimal control volume moving with the fluid (material particle), circumvent some of the problems encountered in higher-order Eulerian closure models. A key advantage to the Lagrangian models is their ability to explicitly account for the particle history and thus their ability to account directly for the coherency in the turbulent transfer within canopies. As in Eulerian models, Lagrangian models vary in complexity as to how the particle trajectory is described in relation to observed features of canopy turbulence. A key disadvantage of Lagrangian models is their inability to compute the velocity field within the flow domain of interest. This, in part, is due to the strong nonlinearity in the resulting equations of motion in the Lagrangian frame of reference [*Monin and Yaglom*, 1971, pp. 531–532].

As discussed in the review by *Raupach* [1988], canopy transport experiments over the last 3 decades clearly demonstrated that canopy turbulence, especially in forests, is (1) inhomogeneous, (2) coherent and persistent with finite integral timescales, and (3) non-Gaussian with vertical velocity skewness values up to -1.5. Early analytic solutions to homogeneous and Gaussian turbulence diffusion problems developed by *Taylor* [1921] yield useful results that clearly demonstrate the important role of coherency in turbulent transport but do not account for the inhomogeneity and non-Gaussian distribution of the velocity statistics. On the other extreme, recent "random walk" and "random flight" models have been proposed to simulate particle trajectory in inhomogeneous [*Horst and Weil*, 1992; *Leclerc and Thurtell*, 1990; *Leclerc et al.*, 1988; *Thomson*, 1987; *Sawford*, 1985; *Ley and Thomson*, 1983; *Wilson et al.*, 1983; *Legg and Raupach*, 1982; *Wilson et al.*, 1981a, b; *Reid*, 1979] and non-Gaussian turbulence [*Sawford*, 1986, 1993; *Wilson and Flesch*, 1993; *Luhar and Britter*, 1989; *Du et al.*, 1994]. However, random flight models suffer from mathematical problems in strongly non-Gaussian turbulence, and the calculations are lengthy and noisy due to the large number of particles and time steps required.

Raupach [1983, 1988, 1989a, b] proposed the "localized near-field theory" or LNF, which is an intermediate class of models between the analytic theories of *Taylor* [1921] for Gaussian homogeneous turbulence and the complex random flight models. The LNF theory is capable of incorporating the nonhomogeneity and persistency of turbulence, but is incapable of incorporating the non-Gaussian distribution of the velocity statistics when compared to random flight models.

Whether LNF is a significant improvement over K theory in practical field applications remains unresolved. Support for the usefulness of LNF is evidenced by the wind tunnel and field experiments presented by *Raupach* [1989a] and *Raupach et al.* [1992]. However, *Van den Hurk and McNaughton* [1995], *McNaughton and Van den Hurk* [1995], and *Dolman and Wallace* [1991] report that the LNF near-field corrections are minor and K theory is adequate for describing mass and heat fluxes from canopies. We note that both the *Dolman and Wallace* [1991] and *Raupach et al.* [1992] field experiments were over short crops (not exceeding 3 m).

The objective of this study is to evaluate the usefulness of LNF in predicting the relationship between the sources and sinks, turbulent fluxes, and mean concentrations of CO_2 in a complex canopy environment such as a forest. An experiment was carried in an 11–13 m tall uniform-aged and managed loblolly pine stand, where profiles of mean CO_2 concentrations, CO_2 turbulent fluxes, and other velocity statistics were measured. The specific objectives of this study are to predict the diurnal variation of CO_2 fluxes from profile measurements and other velocity statistics using LNF, to investigate the CO_2 flux errors resulting from the Gaussian distribution and the neglect of advective transport in LNF, and to compare LNF and K theory CO_2 flux predictions within the forested system.

2. Theory

In the Lagrangian frame of reference, the motion of an infinitesimal material particle of air can be described by

$$X_i(t) = X_i(t_0) + \int_{t_0}^{t} U_i(s)\, ds \tag{4}$$

where X_i $(= X_1, X_2, X_3)$ is the position vector from a preset origin, U_i are the Lagrangian velocity components of the air parcel, and $X_i(t_0)$ is the initial position vector of the air parcel at time t_0. The Navier-Stokes equations describing the time evolution of the Eulerian velocity components can be transformed into the Lagrangian frame of reference [e.g., *Monin and Yaglom*, 1971, pp. 531–532] to obtain an equation for U_i; however, such a transformation results in viscous interaction forces that are described by nonlinear terms of the fifth degree in the variable X_i. Thus the solution to the Lagrangian equations of motion for U_i is much more difficult than their Eulerian counterpart.

In this study an infinitesimal material particle of air (or air parcel) is defined as a tiny connected lump of air containing many molecules of material C and is smaller in size than the smallest eddy size within the canopy [e.g., *Hunt*, 1982]. The smallest eddy is of the order of the Kolmogorov microscale $\eta(=[\nu^3/\langle\varepsilon_{\mathrm{TKE}}\rangle]^{1/4} \sim 1$ mm), where ν is the air kinematic viscosity, and $\langle\varepsilon_{\mathrm{TKE}}\rangle$ is the mean turbulent kinetic energy dissipation rate

per unit mass of fluid. For this air parcel, the conservation of mass for a scalar C, such as CO_2, at position X_i is given by

$$\frac{dC(X_i, t)}{dt} = k_c \frac{\partial^2 C(X_i, t)}{\partial x_i \partial x_i} \tag{5}$$

Hence the air parcel changes its concentration only by molecular diffusion. The Lagrangian dispersion theory within the canopy utilizes the conservation of mass in (5) as follows:

1. Scalar sources and sinks, which are molecular fluxes at the leaf-atmosphere interface, are defined by a source density function $S(X_i, t)$, with dimensions of mass of C per unit mass of air per unit time. At the leaf source locations, $S(X_i, t)$ is nonzero, but it is zero everywhere else. Throughout this study, we refer to $S(X_i, t)$ as a source, but it is understood that $S(X_i, t)$ can be positive (source) or negative (sink).
2. Molecular diffusion in (2) is negligible, so (5) reduces to $dC/dt = 0$, except at the source location where $dC/dt = S(X_i, t)$. That is, once the air parcel is in contact with a source, it changes its concentration, but retains that concentration as it disperses by the turbulent velocity field.
3. The thin laminar boundary layers around individual leaves are considered as part of the source term $S(X_i, t)$. That is, the variation of the leaf boundary layer thickness is small enough so that $S(X_i, t)$ can be treated as a point source relative to the air volume within the canopy.

These assumptions are valid if the airflow inside and above the canopy is at a high enough Reynolds number ($R_e = U_T L_T/\nu$) and Peclet number ($P_e = U_T L_T/k_c$) so that the rate of change of concentration due to molecular diffusion is negligible. Here, U_T and L_T are characteristic turbulent velocity and length scales, respectively.

2.1. Steady Homogeneous Turbulence

In stationary, horizontally homogeneous canopy conditions, the mean concentration of a scalar $C(z, t)$ is related to the statistics of an ensemble of dispersing marked fluid parcels at a given vertical location (z) and time (t) by

$$\langle C(z, t)\rangle = \int\int P(z, t|z_0, t_0) S(z_0, t_0)\, dz_0\, dt_0 \tag{6}$$

where angle brackets denote ensemble averaging, $S(z_0, t_0)$ is a source or sink strength of the scalar from a unit volume of leaves, $P(z, t|z_0, t_0)$ is the transition probability density function that defines the probability of an air parcel released at time t_0 from a position z_0 being observed at time t and position z [see *McComb*, 1990, pp. 436–459]. Since the air parcel concentration directly measures the source strength, (6) states that the ensemble concentration can be interpreted as a weighted average concentration, where the weights are given by the transitional probability density functions. The main challenge in Lagrangian dispersion modeling is to specify $P(z, t|z_0, t_0)$ from readily measured Eulerian velocity statistics. As noted earlier, the solution to the Navier-Stokes equations in the Lagrangian frame of reference can produce the statistics of U_i, but these equations are much more difficult to solve due to the nonlinearity in the viscous forces when compared to their Eulerian counterpart. Hence, within the context of Lagrangian models, the velocity statistics are assumed to be known or can be related to their Eulerian counterpart.

The relation between $P(z, t|z_0, t_0)$ and the velocity statistics was first carried out by *Taylor* [1921] for the case of steady homogeneous turbulence and serves as the main introduction to LNF theory. In the case of steady homogeneous turbulence with zero mean vertical velocity $\langle W(t)\rangle = 0$, the Eulerian velocity statistics are nonbiased samples of the Lagrangian velocity statistics [see *Pasquill and Smith*, 1983, pp. 80–84; *Fischer et al.*, 1979, pp. 60–61; *McComb*, 1990, pp. 447–449]. In this case, if an ensemble of marked air parcels (marked by a tracer such as CO_2) are released from a point source at $t = 0$ and $z = 0$, then the averaged depth at time t of the resulting cloud is related to the velocity statistics by *Taylor*'s [1921] kinematic theorem,

$$\frac{d\sigma_z^2}{dt} = 2\sigma_w^2 \int_0^t R_L(s)\, ds \tag{7}$$

where $\sigma_z = \langle [Z(t) - \langle Z(t)\rangle]^2\rangle^{1/2}$, $R_L(s) = \langle W(t)W(t + s)\rangle/\sigma_w^2$ is the Lagrangian autocorrelation function of $W(t)$ at time lag s, and $\sigma_w^2 = \langle W(t)^2\rangle$ is the root-mean-square Lagrangian vertical velocity, assumed to be identical to the Eulerian vertical velocity variance [*Tennekes and Lumley*, 1972]. The Lagrangian autocorrelation function is well approximated by an exponential form [*Snyder and Lumley*, 1971] and is given by

$$R_L(s) = \exp(-s/T_L) \tag{8}$$

where T_L is the Lagrangian integral timescale [*Tennekes and Lumley*, 1972, pp. 229–230; *Csanady*, 1973; *Corrsin*, 1963]. Hence (7) can be solved for $\sigma_z(t)$ to give

$$(\sigma_z(t))^2 = 2\sigma_w^2 T_L^2 \left(\frac{t}{T_L} - 1 + \exp(-t/T_L)\right) \tag{9}$$

In a steady homogeneous flow the distributions of $W(t)$ and $Z(t)$ are both Gaussian, so the transition probability density function $P(z, t|0, 0)$ is determined by

$$P(z, t|0, 0) = \left(\frac{1}{\sqrt{2\pi}\,\sigma_z(t)}\right) \exp\left(-\frac{Z(t)^2}{2\sigma_z(t)^2}\right) \tag{10}$$

Since $\sigma_z(t)$ is related to the velocity statistics by (9), (10) shows how the transition probability density function is explicitly related to the velocity statistics. Also, as discussed by *Raupach* [1988], (9) suggests that the turbulence dispersion follows different dynamics in the limits when $t \gg T_L$ and $t \ll T_L$. That is,

$$\begin{aligned} \sigma_z(t) &= \sqrt{2}\,\sigma_w T_L \left(\frac{t}{T_L} - 1\right)^{1/2} \qquad t/T_L \gg 1 \\ \sigma_z(t) &= \sqrt{2}\,\sigma_w T_L \left(\frac{t}{T_L}\right) \qquad t/T_L \ll 1 \end{aligned} \tag{11}$$

Hence, when the travel time is large (far field), the dispersion of particles by turbulence produces a cloud with depth increasing as $t^{1/2}$. Thus the turbulence dispersion in the far field can be described as diffusive. This is not the case for small t/T_L (near field), where the cloud depth defining the mean trajectory grows linearly with time next to the source (see Figure 1a; also see *Raupach* [1989a]). Hence the turbulence dispersion in the near field close to a source is considered nondiffusive. Within the near field the travel time is smaller than the integral timescale, and hence $S(z, t)$ variability within the canopy volume significantly contributes to the mean concentration due to turbulence persistence and finite integral timescales. In the far field, persistence is not significant and turbulence is diffusive. This is the essence of LNF theory as derived by *Raupach* [1983, 1988, 1989a, b]. Much of the material below is presented

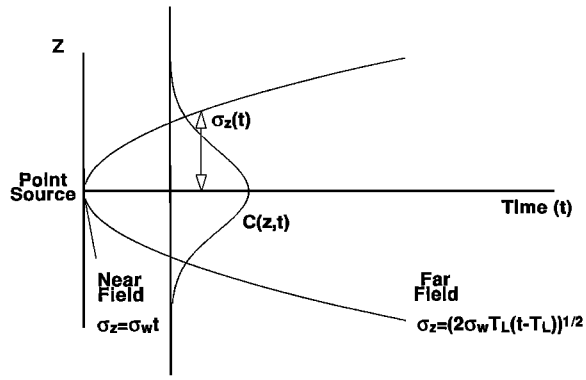

Figure 1a. Definition of Lagrangian variables.

by *Raupach* [1989a, b]. For completeness, we review the main steps in the derivation of LNF to highlight key assumptions that are known to be violated within the plant canopy environment.

2.2. Localized Near-Field Theory

The CO_2 in a canopy is being emitted (or absorbed) by a large number of point sources or sinks at the organ scale (leaf, branch, or stem section) inside the canopy volume. The leaves per unit volume are approximated by point sources or sinks relative to the airflow inside the canopy. The plumes emitted from each leaf volume pass through both the near-field and far-field dispersion regimes; hence at a tower or measurement location inside the canopy, plumes at all stages of evolution occur, and the concentration is the superposition of all these plumes (see, e.g., Figure 1b and *Kaimal and Finnigan* [1994, p. 92]). The near-field contribution to the dispersion occurs at timescales up to T_L. In order to relate this timescale to a physical dimension, we note that within a canopy of height h, $T_L \sim h/\sigma_w$, and $\langle U \rangle \sim \sigma_w$, so an estimate of the maximum travel distance that will be significantly influenced by the near field is $\langle U \rangle T_L \sim h$. Hence all leaves that are within a distance h from the measurement point will contribute, in a nondiffusive manner, to the mean concentration at that point.

The LNF theory derives $P(z, t|z_0, t_0)$ for nonhomogeneous turbulence as a function of the velocity statistics accounting for near- and far-field differences in dispersion regimes. For that purpose, *Raupach* [1989a, b] decomposed the transition probability density function into two components,

$$P(z, t|z_0, t_0) = P_f(z, t|z_0, t_0 + T_L) + P_n(z, t|z_0, t_0) \tag{12}$$

where P_f and P_n are the far-field and the near-field transition probability density functions, respectively. In order to arrive at an analytic description of the transition probability density function, *Raupach* [1989a, b] suggested constructing a purely artificial diffusive plume that (1) is identical to the real dispersion cloud at the far field (i.e., $P(z, t|z_0, t_0) = P_f(z, t|z_0, t_0)$), and (2) best matches P_n for timescales comparable to T_L (although LNF cannot exactly match P_n). Since P_n is unknown for inhomogeneous turbulence, Raupach suggested estimating P_n assuming locally homogeneous turbulence with a velocity and timescale $\sigma_w(z_0)$ and $T_L(z_0)$ using the analytic theory of *Taylor* [1921]. The best match between this artificial diffusive cloud and the real cloud is when $P(z, t|z_0, t_0)$ approaches $P_f(z, t|z_0, t_0)$ as $(t - t_0)/T_L$ becomes very large, and $P(z, t|z_0, t_0)$ approaches $P_n(z, t|z_0, t_0)$ when $(t - t_0)/T_L$ is much smaller than unity. Since $P_n(z, t|z_0, t_0)$ is unknown, it can be approximated by its value determined in a locally homogeneous turbulence with velocity and timescales $\sigma_w(z_0)$ and $T_L(z_0)$. For homogeneous turbulence both $P(z, t|z_0, t_0)$ and $P_f(z, t|z_0, t_0)$ are known from the analytic results of *Taylor* [1921], and thus $P_n(z, t|z_0, t_0)$ can be determined. That is, LNF does not explicitly account for the nonhomogeneity in turbulence for determining P_n. Within the canopy the turbulence is not homogeneous, and σ_w and T_L vary with height. To account for this nonhomogeneity in the far field, *Raupach* [1989a] suggested that K_f be replaced by $K_f(z) = \sigma_w(z)^2 T_L(z)$. This approximation is satisfactory for near-neutral conditions and in plant canopies, but is unsatisfactory for convective boundary layers. Numerical simulations using *Sawford*'s [1986] random flight approach suggest that this K_f approximation is valid if $d[(\sigma_w(z)T_L(z)]/dz$ does not exceed 0.4 (i.e., when the turbulence is weakly inhomogeneous). It is exact for homogeneous turbulence.

Next, we consider an extensive canopy with negligible advection so that a balance between the turbulent flux through a plane parallel to the ground surface at height z from the ground and the source profile is given by

$$F_c(z) = F_c(0) + \int_0^z S(z)\, dz \tag{13}$$

where $F_c(z) = \langle wc \rangle$ is the turbulent flux at height z, and $F_c(0)$ is the ground flux. For this canopy, analogous to the transition probability density function, the mean concentration can also be decomposed into a far-field $C_f(z, t)$ and a near-field $C_n(z, t)$ so that

$$C(z, t) = C_f(z, t) + C_n(z, t)$$

$$C_f(z, t) = \int_0^\infty S(z_0) \int_0^{t - T_L(z_0)} P_f(z, t|z_0, t + T_L(z_0))\, dt_0\, dz_0 \tag{14}$$

$$C_n(z, t) = \int_0^\infty S(z_0) \int_0^t P_n(z, t|z_0, t_0)\, dt_0\, dz_0$$

Based on the previously proposed idealized diffusive cloud, *Raupach* [1983; 1989a, b] showed that the far-field and near-field concentrations are best matched if

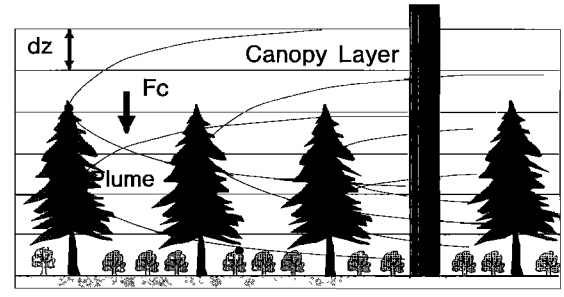

Figure 1b. Conceptual framework for the application of Lagrangian models in forested ecosystems from *Kaimal and Finnigan* [1994].

$$C_f(z) = C(z_R) - C_n(z_R) + \int_s^{z_R} [F(z)/K_f(z)]\, dz$$

$$C_n(z) = \int_0^{\infty} \frac{S(z_0)}{\sigma_w(z_0)} \left[k_n\left(\frac{z - z_0}{\sigma_w(z_0) T_L(z_0)} \right) + k_n\left(\frac{z + z_0}{\sigma_w(z_0) T_L(z_0)} \right) \right] \quad (15)$$

$$k_n(x) = \frac{1}{\sqrt{2\pi}} \int_0^{\infty} \frac{\exp(-s)}{\sigma(s)} \exp\left(\frac{-x^2}{2\sigma^2(s)} \right) ds$$

$$\approx -0.39894 \ln[1 - \exp(-|x|)] - 0.15623 \exp(-|x|)$$

where k_n is a near-field kernel function, and the approximation to k_n in (15) is derived by *Raupach* [1989b]. Though this artificial diffusion cloud does not match the true near field for nonhomogeneous turbulence within the plant canopy, it does account for near-field effects on the mean concentration had the turbulence been locally homogeneous with a velocity $\sigma_w(z_0)$ and timescale $T_L(z_0)$. This completes the Lagrangian description of the relationship between $S(z)$, $C(z)$, and $F(z)$. Notice in (15) that if $S(z)$, $\sigma_w(z)$, and $T_L(z)$ are known, $F(z)$ can be estimated from (13), and the concentration profile can be estimated from (14) and (15). This approach was called the "forward problem" by *Raupach* [1989a].

The "inverse problem" is defined as follows: given $\sigma_w(z)$, $T_L(z)$, and $C(z)$ (rather than $S(z)$), can we use (13), (14), and (15) to solve for $S(z)$ and $F(z)$. It is this "inverse" problem that is of interest in practice, since $S(z)$ cannot be directly measured in forested canopies. The solution of the inverse problem is considered next.

2.3. The Inverse LNF Problem

In practice, profile measurements are made at discrete layers, and thus the solution to the inverse problem is done in a discrete form. In this section we review the key steps in the work by *Raupach* [1989a] of how to use discrete concentration measurements to predict $S(z)$ and $F(z)$ in conjunction with either measured or assumed profiles of $\sigma_w(z)$ and $T_L(z)$ within and above the canopy.

1. The canopy is divided into m horizontal layers, each having a uniform source density S_j over dz_j ($=z_j - z_{j-1}$), where $j = 1, \cdots, m$. Any scalar flux originating from the ground is lumped with the source term from the lowest layer.

2. The concentration measurements C_i within and above the canopy are available at n measurement heights ($i = 1, \cdots, n$).

3. The $\sigma_w(z)$ and $T_L(z)$ profiles within and above the canopy are measured or estimated. While both of these statistics are Lagrangian quantities, they may be estimated from Eulerian velocity and integral timescale statistics. This will be further discussed in the results and discussion section. For the purpose of this section, it is assumed that $\sigma_w(z)$ and $T_L(z)$ are known.

4. A dispersion matrix is computed from

$$D_{ij} = \frac{c_i - c_R}{S_j\, dz_j} \quad (16)$$

as follows: Place a unit source at height z_1, and compute the resulting concentration profile c_i at all heights z_i for $i = 1$ to n relative to the reference height c_R. Repeat the calculations by placing the unit source at $z_2, z_3, \cdots, z_m$ until all elements of the dispersion matrix D_{ij} are computed. The estimation of the concentration profile from each unit source is carried out using the LNF formulation described in (13), (14), and (15) with the given profiles of $\sigma_w(z)$ and $T_L(z)$ and a unit S as input (the forward problem). It should be noted that the far-field concentration is estimated by neglecting longitudinal advection within the canopy. This assumption will be evaluated in the results and discussion section.

5. Once D_{ij} is known, the concentration profile and the source profile S_j can be determined by the superposition principle. This principle states that if source densities S_1 and S_2 produce concentration fields C_1 and C_2, then a source density $S_1 + S_2$ produce a concentration field $C_1 + C_2$ [also *Monin and Yaglom*, 1971, pp. 591–606]. More formally,

$$C_i - C_R = \sum_{j=1}^{j=m} D_{ij} S_j\, dz_j \quad (17)$$

If $m = n$, the above equation involves solving m linear equations with m unknowns for the source profile (S_j; $j = 1, \cdots, m$), since the dispersion matrix D_{ij} and C_i are known. The flux profile can be estimated from (13). *Raupach* [1989a] noted that the solution to this system is very sensitive to small errors in the concentration measurements or the estimation of $\sigma_w(z)$ and $T_L(z)$. Hence one approach to overcome this difficulty is to include some redundant concentration data in the estimation of S_j from C_i, such that the m source strength densities are estimated from n concentration measurements with $m < n$. Hence *Raupach* [1989a] proposed a least squares approach that best describes the measured C_i profile ($i = 1, \cdots, n$) from S_j ($j = 1, \cdots, m$) by minimizing the squared error

$$\varepsilon = \sum_{i=1}^{n} (C_i - \hat{C}_i)^2 \quad (18)$$

where ε is the mean square error in the predicted profile (C_i) from S_j, and $\hat{C}_i$ is the measured concentration profile. Replacing (18) in (17),

$$\varepsilon = \sum_{i=1}^{i=n} \left[\sum_{j=1}^{j=m} D_{ij} S_j\, dz_j - (\hat{C}_i - C_R) \right]^2 \quad (19)$$

The values S_j that minimize ε are given by

$$\frac{\partial \varepsilon}{\partial S_j} = 0 \qquad j = 1, 2, \cdots, m \quad (20)$$

which results in m linear equations with m unknowns ($= S_j$). These equations are of the form

$$\sum_{k=1}^{k=m} A_{jk} S_k = B_j, \qquad j = 1, \cdots, m$$

$$A_{jk} = \sum_{i=1}^{i=n} D_{ij}\, dz_j\, D_{ik}\, dz_k \quad (21)$$

$$B_j = \sum_{i=1}^{i=n} (\hat{C}_i - \hat{C}_R) D_{ij}\, dz_j$$

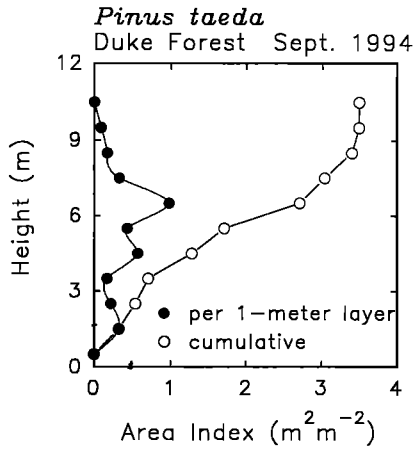

Figure 2. The measured cumulative and actual leaf area index (LAI) profile at the tower facility.

Hence using the measured $\hat{C}_i$, and by estimating D_{ij} from $\sigma_w(z)$ and $T_L(z)$, S_j can be determined by solving the above m equations. Since S_j is estimated, F_c can be computed from

$$S_j = \frac{F_j - F_{j-1}}{dz_j} \tag{22}$$

This completes the review of the LNF "inverse problem" in the absence of advective transport as outlined by *Raupach* [1989a].

3. Experiment

In order to investigate the usefulness of LNF to predict sources and fluxes of CO_2 in forests, an experiment was carried out on September 19, 1994. The site is a 1000 m × 300 m 12 year old managed *Pinus taeda L.* (loblolly pine) stand patch within the Blackwood division of the Duke Forest in Durham, North Carolina (35°98′N, 79°8′W, elevation = 163 m). Further details about the site and understory species composition can be found in the work by *Ellsworth et al.* [1995]. The site is equipped with a 20 m walkup tower situated some 100 m from the southern edge and 50 m from the western edge. The measurements consisted of (1) CO_2 mean concentration profiles, (2) CO_2 eddy correlation fluxes at z = 9 m, and (3) supporting turbulent velocity statistics within and above the canopy.

The three velocity components (U_1, U_2, U_3) and air temperature (T) were measured using a Gill triaxial ultrasonic anemometer at 13 m above the ground surface (see *Katul* [1994] and *Katul et al.* [1995] for anemometer details). The sonic path of the Gill anemometer is 0.149 m. The measurements were corrected for transducer shadowing effects and rotated so that the U_1 is aligned along the mean longitudinal wind direction at the canopy top every 20 min. Two Campbell Scientific (CA27) one-dimensional sonic anemometers, situated at 9 m and 14 m above the ground surface, were also available during this experiment and provided direct measurements of T_E and σ_w. The CA27 sonic inside the canopy was situated at least 60 cm (4 times the path length) from the nearest leaf to avoid any potential interferences between the reflected sonic wave from the CA27 sonic transducer and the waving motion of the leaves.

A fast response LICOR 6262 CO_2/H_2O gas analyzer with 10 Hz sampling capability was used to sample the CO_2 concentration at 9.0 m using a 10 L min^{-1} flow rate. The peak-to-peak noise level for the CO_2 output channel was below 0.3 ppm. A Campbell Scientific Krypton hygrometer (KH_2O), colocated with the CA27 at 9.0 m, was used to check tube attenuation and lag response time of the LICOR 6262 water vapor signal. Appendix A presents a comparison between the two water vapor measurements and the lag time corrections applied to the CO_2 time series prior to estimating the covariance between the CO_2 concentration and the CA27 vertical velocity time series.

The measurements of CO_2 profiles were carried out using a LICOR 6252 gas analyzer at six elevations (1, 3, 6, 9, 12, and 19.5 m), sequentially. The concentration measurement at each level required 1.25 min dwell time in order to purge the existing air and for the gas analyzer to determine the 1 min average CO_2 concentration. In order to insure steadiness in the mean meteorological conditions, the CO_2 concentration profile data were averaged every 20 min (three measurements per level). Due to the availability of two CO_2 measurements at 9.0 m, a comparison between the mean CO_2 concentration obtained from the 10 Hz LICOR 6262 (N = 12,000 points) instrument and the CO_2 LICOR 6252 gas analyzer was carried out in Appendix B.

A 21X Campbell Scientific micrologger was used to sample the five analog velocity signals, the Gill triaxial sonic anemometer temperature signal, the KH_2O Krypton hygrometer signal, and the two LICOR 6262 CO_2/H_2O signals at 10 Hz. The data from the 21X were transferred via an optically isolated RS232 interface (Campbell Scientific SC32A) to a portable personal computer and stored on a hard drive for future processing. While the 50 m fetch was small for southerly wind conditions, the winds above the canopy were predominantly from the north for this day. Also, it should be noted that the eddy correlation measurements were performed inside the canopy and the fetch was not as critical as for surface layer experiments.

The shoot silhouette area index, a value analogous to the leaf area index (LAI), was measured in the vertical by a pair of LICOR LAI 2000 plant canopy analyzers on September 9, 1994, and is shown in Figure 2. The data in Figure 2 were not corrected for foliage aggregation as can be common in conifer trees. Hence the values are only used for qualitive comparisons with the LNF-predicted source/sink profiles. Notice in Figure 2 that three peaks in the LAI profile are evident, but the maximum LAI is at 6.5 m. Also, from Figure 2, the LAI contribution of the understory is significant relative to the overall LAI.

The CO_2 profiles and turbulence statistics measurements were used to estimate the mean source strength and turbulent flux profiles. The predicted CO_2 turbulent fluxes were compared with direct eddy correlation measurements on a 20 min time step throughout the day.

4. Results and Discussion

4.1. Estimation of σ_w and T_L Profiles

The vertical velocity variance profile was determined every 20 min from the velocity measurements as follows: (1) For $z >$ 14 m, a constant value identical to the measured value at z = 14 m was used. (2) For $z >$ 9 m and $z <$ 14 m, a linear interpolation between the measurements was carried out. (3) For $z >$ 0 and $z <$ 9 m, a linear functional form was used between the measured values at 9 m ($\sigma_w(9)$) and an estimated $\sigma_w(0) = 0.3\sigma_w(9)$. The factor 0.3 was determined from *Raupach* [1988]. It is assumed that these Eulerian vertical velocity measured statistics are unbiased samples of the Lagrangian values [*Pasquill and Smith*, 1983]. We also compared

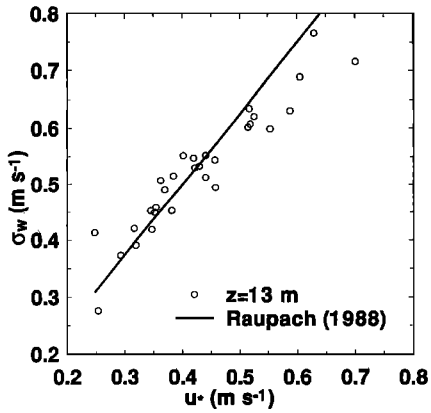

Figure 3a. The relationship between measured σ_w ($= \langle w^2 \rangle^{1/2}$) and u_* at $z/h = 1$. The solid line is $\sigma_w = 1.25u_*$, which is the best fit line to the measurements in the work by *Raupach* [1988].

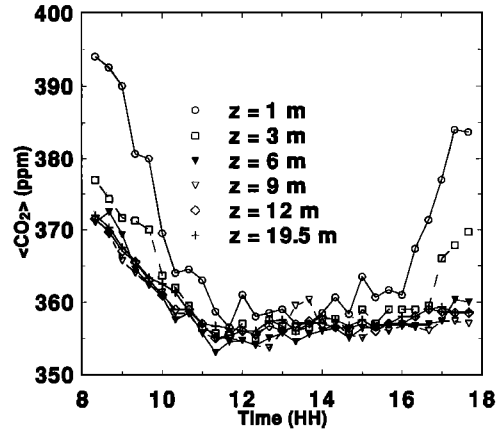

Figure 3c. Similar to Figure 3b, but for the mean CO_2 concentration at six levels.

our measurements with the measurements reported by *Raupach* [1988] for $z/h = 1.0$ by comparing the relationship between σ_w and u_* in Figure 3a. Good agreement is noted in Figure 3a between measurements and the similarity relationship $\sigma_w = 1.25u_*$, confirming the suitability of this relationship for a wide range of surface conditions.

The integral timescale was assumed to be constant with height as in the work by *Raupach* [1988] and identical to the value above the canopy. The value above the canopy was determined by

$$T_L = \beta T_E^{(\text{avg})}$$
$$\beta = \frac{\alpha \langle U \rangle}{\sigma_w} \tag{23}$$

where $\alpha \approx 1$ and T_E is the Eulerian integral timescale determined from

$$T_E = \int_0^\infty \rho_E(s)\, ds$$
$$\rho_E(s) = \frac{\langle w(t+s)w(t) \rangle}{\sigma_w^2} \tag{24}$$

where $\rho_E(s)$ is the Eulerian vertical velocity autocorrelation function. In practice, the above integration was carried out up to the first zero crossing (see Appendix C). The value of α was assumed to be height-independent. The average Eulerian integral timescale was determined from the vertical velocity time series measurements by averaging the measured T_E at 9, 13, and 14 m. In order to compare with *Raupach* [1988], we computed the dimensionless timescale $T^* = (u_* T_L)/h$ for all the runs in Figure 3b. The horizontal dashed line is the mean value of the data of *Raupach* [1988]. The agreement is within the scatter displayed by *Raupach* [1988].

4.2. Predictions of CO_2 Sources and Fluxes Using LNF

In order to predict CO_2 scalar sources and fluxes using LNF, two sets of inputs are required: (1) the mean CO_2 concentration profile within and above the canopy; and (2) the profiles of σ_w and T_L. A vertical grid with $dz = 0.25$ m was first constructed, resulting in 80 nodes. A fine-resolution grid (0.25 m) was necessary since the flux was computed by integrating the source profile as in (13). The 80 nodes were a good compromise between a fine grid size and the potential instabilities resulting from the Gauss-Jordan elimination method for in-

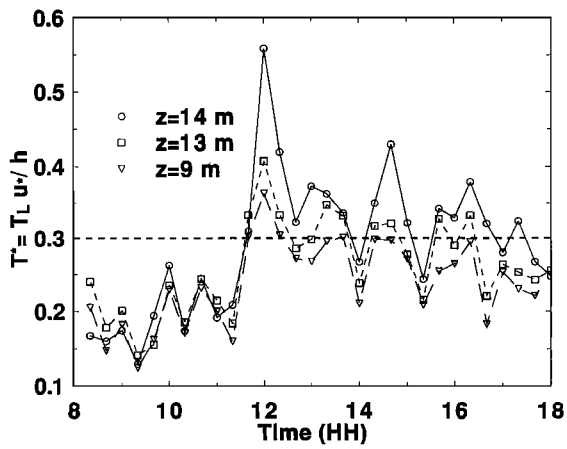

Figure 3b. The diurnal variation of the dimensionless canopy timescale $T^* = u_*(\beta T_E)/h$; $\beta = \alpha\langle U \rangle/\sigma_w$, and $\alpha = 1$, $h = 13$ m. The horizontal dashed line is the mean value of T^* from a wide range of experiments reported by *Raupach* [1988].

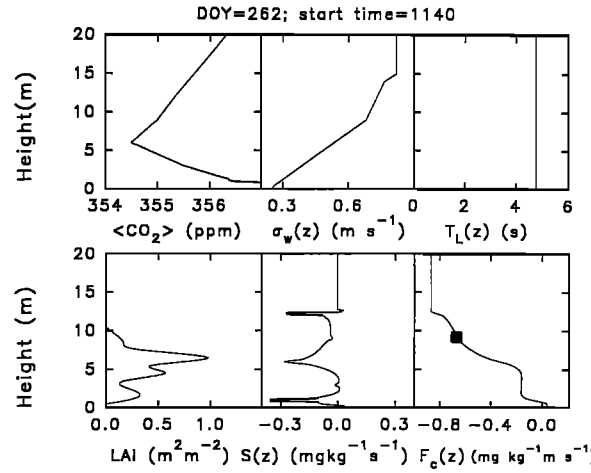

Figure 3d. The assumed profiles of C, σ_w, T_L (time, 1140). The LNF predicted source and flux profiles are presented. The LAI profile is also shown for qualitative comparison with the source profile.

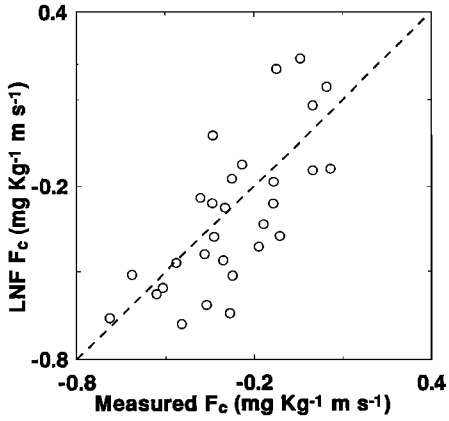

Figure 4. Comparison between eddy correlation measured and LNF predicted averaged 20 min CO_2 fluxes. The 1:1 line is also shown ($r^2 = 0.58$).

verting matrices [see *Press et al.*, 1992, pp. 22–34]. The mean CO_2 concentration profiles at these nodes were determined from linear interpolation between the six measurement levels shown in Figure 3c. Notice in Figure 3c that the highest CO_2 concentration values occur close to the ground surface except between hours 13 and 14. We note that interpolating between concentration measurements departs from the suggestions by *Raupach* [1989a], who assumed that the source profile was constant across dz, where dz is determined from the measurement grid. In Appendix D, we further explore the consequences of assuming a continuous concentration profile vis à vis Raupach's discontinuous source profile.

The dispersion matrix D_{ij} with $i = 1, \cdots, 80$ and $j = 1, \cdots, 52$ was constructed using (16) by placing a unit source strength at $j = 1, \cdots, 52$ and using the forward LNF defined by (13), (14), and (15). The ground was assumed to be a source of CO_2, and thus the concentration at the ground level was assumed to be the same as the value at $z = 1.0$ m. Once D_{ij} is calculated for each 20 min time step, the source profile is computed from (17) and the flux profile is computed from (13). As an illustration, Figure 3d shows the 20 min mean variation of C, σ_w, and T_L with height (start time, 1140). The LNF model was used to predict the source and flux profiles $S(z)$ and $F(z)$. For reference purposes, the LAI profile is also shown. Notice the close correspondence between the LAI and the S profile. Clearly, the near-field contribution to the C profile must be responsible for such a close relation between the LAI and S. Also, it is interesting to note in Figure 3d that LNF predictions did reproduce (1) the countergradient transport at $z = 8$ m, (2) the fact that the near-ground air is a CO_2 source, and (3) the fact that the maximum CO_2 source is at the canopy-atmosphere interface and that the point of maximum LAI is the point of maximum CO_2 sink.

4.3. Comparisons Between LNF Flux Predictions and Eddy Correlation Measurements

A comparison between measured and predicted CO_2 fluxes is shown in Figure 4. A linear regression model of the form $F_c^{(ec)} = AF_c + B$ was used to assess the model performance. Here, $F_c^{(ec)}$ is the eddy correlation measured flux, and F_c is the LNF predicted flux. The coefficient of determination ($r^2 = 0.58$) and the standard error of estimate (SEE = 0.16 mg kg^{-1} m s^{-1}) suggest that the modeled and measured CO_2 fluxes at $z = 9$ m are in good agreement.

4.4. Error Analysis

As was noted in the theory section, two key assumptions must be satisfied in the LNF formulation: (1) the canopy flow is purely dispersive with no advective transport, and (2) the distribution of the vertical velocity is near-Gaussian. In order to check how significant these simplifications are on the LNF estimated flux, an error analysis was carried out. For that purpose, the error in the 20 min CO_2 fluxes at 9 m (ε_F) was computed by

$$\varepsilon_F = F_c^{(\mathrm{LNF})} - F_c^{(\mathrm{ec})} \tag{25}$$

where $F_c^{(\mathrm{LNF})}$ and $F_c^{(\mathrm{ec})}$ are the LNF predicted and eddy correlation measured CO_2 fluxes. In order to evaluate the influence of the above two assumptions on the LNF flux predictions, we consider the following relations: (1) If the advective transport significantly affects the LNF flux predictions, then ε_F and the mean longitudinal velocity $\langle U \rangle$ at the canopy top must be strongly correlated. (2) If the near-Gaussian approximation significantly affects the LNF flux predictions, then ε_F and the vertical velocity skewness and flatness factors at 9 m must be strongly correlated.

These two points are considered in Figures 5a, 5b, and 5c. In Figure 5a, ε_F as a function of $\langle U \rangle$ is shown along with the regression line. No significant trend at the 95% confidence limits was observed, suggesting that the errors in neglecting advective transport are not very significant for this experiment. However, Figure 5b does suggest that the skewness has some marginal effects on the LNF estimated CO_2 flux. The regression slope was statistically significantly different from zero at the 95% confidence interval. As the measured skewness approaches zero (Gaussian), ε_F marginally diminishes (though interestingly the trend is opposite to that in Figure 5a). We note that for strictly homogeneous turbulence, the velocity field is Gaussian [*Batchelor*, 1953, pp. 169–174]. In Figure 5c, ε_F varied mildly with the flatness factor. Recall that for a Gaussian distribution, the flatness factor is 3. These two findings are consistent with the findings from a random flight numerical experiment carried out by *Raupach* [1988] using *Sawford*'s [1986] model.

Finally, the sensitivity of LNF to the choice of α was tested. Recall in (24) that α was assumed to be unity. However, the value of α is not well defined and has been the subject of theoretical and experimental treatments for the past 30 years. *Tennekes and Lumley* [1972, p. 277] proposed an $\alpha = 4/3$ based on the relationship between the Lagrangian and Eulerian velocity spectra in the inertial subrange; *Snyder and Lumley* [1971] found that $\alpha = 1$ from direct measurements of the Eulerian and Lagrangian integral timescales; while the balloon data of *Angell* [1974] and *Pasquill and Smith* [1983, p. 87] suggest an α that can vary from 1 to 2. For that purpose, α was varied from 1 to 2 in increments of 0.2. For each α value, the root-mean-square error $\langle \varepsilon_F^2 \rangle$ was computed for the whole day by averaging the squared error for all 30 measurements. The variation of $\langle \varepsilon_F^2 \rangle^{1/2}$ as a function of α is shown in Figure 5d. Notice that the minimum error occurs at $\alpha = 1$, and increases linearly with increasing α. Hence the recommended α for canopy transport is unity, in agreement with *Raupach*'s [1988] suggestions.

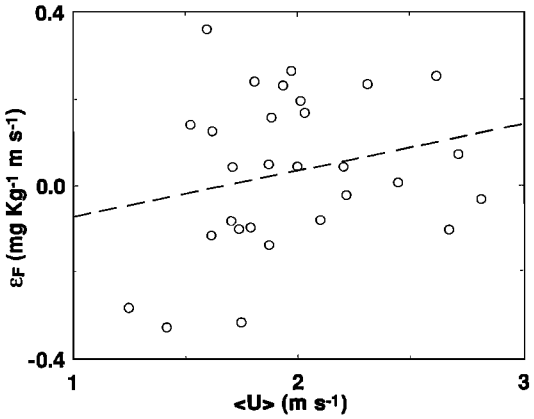

Figure 5a. The CO_2 flux error ε_F as a function of measured longitudinal velocity ($\langle U \rangle$) at z = 13 m. LNF model neglects advection.

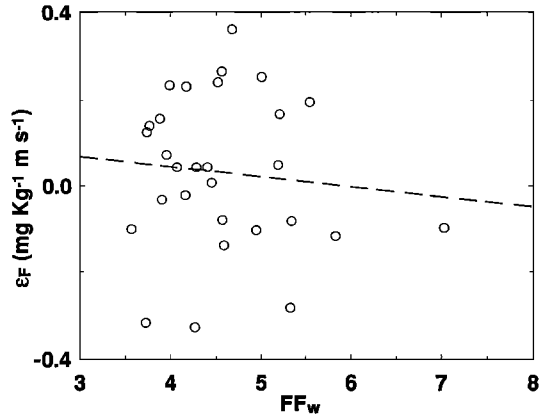

Figure 5c. The CO_2 flux error ε_F as a function of measured vertical velocity flatness factor at z = 9 m. LNF model assumes that the flatness factor is 3.

4.5. LNF, *K* Theory, and Near-Field Dispersion

In order to demonstrate the importance of near-field effects, we compare the CO_2 fluxes predicted from LNF with fluxes predicted using $K(z) = K_f(z) = \sigma_w(z)^2 T_L(z)$ (analogous to K theory with K being defined by the far-field eddy diffusivity) and fluxes measured with the eddy correlation in Figure 6. That is, for K theory, the near-field contribution is set to zero (as suggested by *Dolman and Wallace* [1991], *McNaughton and Van den Hurk* [1995], and *Van den Hurk and McNaughton* [1995]). It is evident that LNF predictions are much more consistent with the eddy correlation measurements when compared with K theory. This is very analogous to the arguments and measurements presented by *Thurtell* [1989]. In the study by *Thurtell* [1989], a small box containing two gases which are diffusing in opposite directions is used; the concentration profile for one of the gases is measured. It was concluded by the author that near the source, K theory cannot reproduce the measured flux, while away from the source (3 to 4 diffusion length scales), K theory accurately predicts the fluxes. We also compared the mean daily CO_2 fluxes measured by the eddy correlation (-0.27 mg kg^{-1} m s^{-1}) and predicted by LNF (-0.30 mg kg^{-1} m s^{-1}) and K theory (-0.43 mg kg^{-1} m s^{-1}). It appears that at such a time step, the LNF is also in better agreement with the eddy correlation when compared to K theory, though further testing is required.

5. Conclusions

This study has focused on the relationship between the CO_2 concentration, source, and flux profiles in a homogeneous loblolly pine stand using a Lagrangian dispersion model originally developed by *Raupach* [1989a, b]. The model inputs included estimates of the Lagrangian integral timescale profile, Lagrangian vertical velocity variance profile, and the mean CO_2 concentration profile. The Lagrangian integral timescale was estimated from measured Eulerian integral timescales within and above the canopy, and the Lagrangian vertical velocity variance was assumed identical to the Eulerian value [see *Corrsin*, 1959]. From these inputs, the source (or sink) profile was computed, and the flux profile inside the canopy was estimated by numerical integration of the source (or sink) profile. The CO_2 flux predictions from this model were compared to direct eddy correlation measurements available at z/h = 0.75. Our study demonstrated the following:

1. The localized near-field (LNF) theory proposed by *Raupach* [1983, 1988, 1989a, b] is an operational method for de-

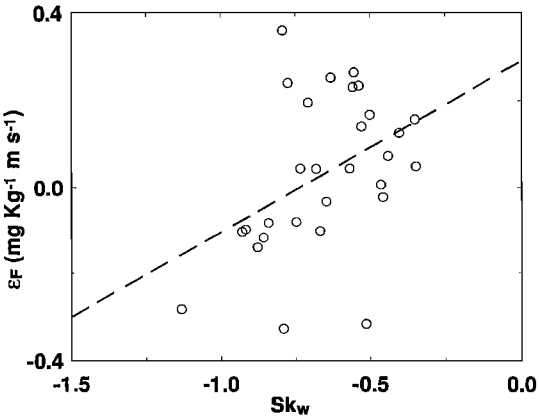

Figure 5b. The CO_2 flux error ε_F as a function of measured vertical velocity skewness at z = 9 m. LNF model assumes a zero skewness.

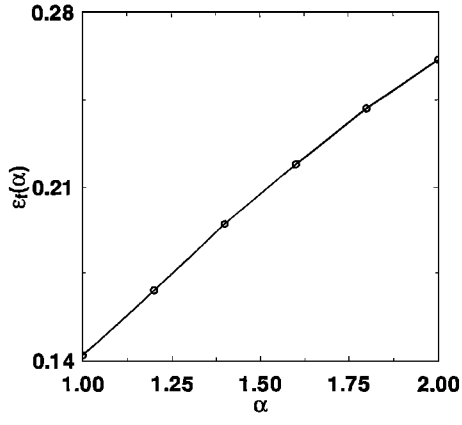

Figure 5d. The CO_2 root-mean-square flux error for all 30 points as a function of α. The α range represents lower and upper limits measured or predicted from laboratory and field experiments.

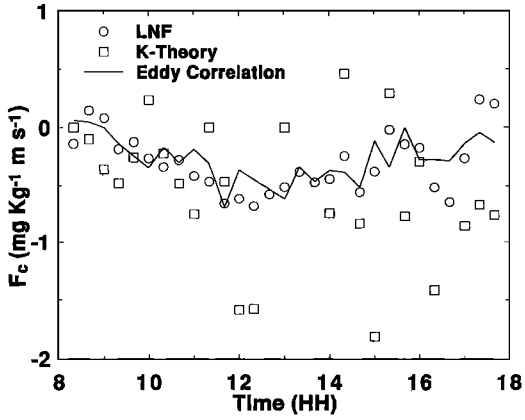

Figure 6. Diurnal variation of eddy correlation measured CO_2 flux, and predicted CO_2 fluxes from LNF and K theory.

scribing sources and fluxes of CO_2 within forested systems if adequate information about the velocity statistics is available.

2. The LNF theory simulated the diurnal variation of the eddy correlation measured CO_2 fluxes better than K theory, suggesting that near-field corrections might be important for canopy transport and forest biosphere-atmosphere interactions. This result appears to be at variance with the conclusions of *Van den Hurk and McNaughton* [1995], *McNaughton and Van den Hurk* [1995], and *Dolman and Wallace* [1991]. This apparent difference may be attributed to the fact that (1) these authors utilized the equivalent of the "forward" LNF approach while our study considered the "inverse" LNF approach, and (2) the comparisons between measured and predicted CO_2 fluxes are within rather than above the canopy. In the forward approach, the near-field concentration corrections are minor, and the flux calculation becomes independent from the dispersion model as in (13). However, in the "inverse" LNF approach, the near-field contribution to the gradient is large [e.g., *Van den Hurk and McNaughton*, 1995, Figure 3].

3. The disparity between predictions based on LNF and eddy correlation measurements decreases as the averaging time period increases. The cumulative fluxes predicted by LNF and measured by eddy correlation are very similar.

4. The absence of the advective transport in LNF is reasonable for within-canopy flux calculations.

5. The departures from non-Gaussian distribution in the vertical velocity marginally influence the LNF model performance. Our study suggests that departures from Gaussian distribution in the odd moments (e.g., skewness) are more important for LNF CO_2 flux estimation than departures in the even moments (flatness factor).

Appendix A: LICOR 6262 Lag Time Corrections

Due to the tubing length between the CO_2 intake and the gas analyzer, the CO_2 concentration measurements lag the one-dimensional sonic anemometer vertical velocity measurements. In order to minimize the influence of this lag and determine its value, the following was carried out:

1. The LICOR 6262 gas analyzer was placed at the top of the tower (12 m vertical distance) away from the CO_2 intake. This minimizes the tubing length between the air intake and the LICOR 6262 gas analyzer. The airflow rates to the LICOR 6262 were 9–10 L min^{-1}.

2. A Campbell Scientific Krypton hygrometer was colocated with the LICOR 6262 gas analyzer. The water vapor time series measurements (sampling rate, 10 Hz) from both instruments were compared every 20 min (N = 12,000 points).

The lag time between the LICOR 6262 gas analyzer and the Krypton hygrometer was determined from the cross-correlation CC(s) function between the LICOR 6262 gas analyzer (q_{ga}) and the Krypton hygrometer measurement (q_{kh}) using

$$\mathrm{CC}(s) = \frac{\langle q_{ga}(t) q_{kh}(t+s) \rangle}{\sigma_{ga}\sigma_{kh}} \tag{26}$$

where s is the time lag. The value of s at which CC(s) is maximum (s_{opt}) determines the optimal lag to be applied to the CO_2 concentration time series in the eddy correlation CO_2 flux measurements. Figure 7a shows the time evolution of the optimal lag (s_{opt}) during the day for every 20 min, as well as the value of CC(s_{opt}) at that time lag. Notice that CC(s_{opt}) exceeded 0.93 for most conditions. The small differences can be attributed to (1) the smearing of high-frequency fluctuations within the tube and (2) the marginal differences in air volumes being sampled since the Krypton was 20 cm away from the gas analyzer air intake.

Appendix B: Adequacy of the Profile Sampling Duration

One main difficulty in measuring the mean vertical CO_2 concentration profiles is the need to resolve very small differences in mean concentration measurements within the canopy. One possible method to achieve this goal is to place many LICOR 6252 gas analyzers (one analyzer per measurement level) calibrated prior to the experiment. Both economy and the unavoidable instrumentation drifts preclude that option. Alternatively, one may sample the CO_2 concentration sequentially with the same gas analyzer at many levels, and repeat this process several times over a sampling period that is short enough to insure stationarity in the mean meteorological conditions. While this profile-sampling method is economical, eliminates the instrument drift problem, and does not require the high instrument precision needed in the first alternative, it

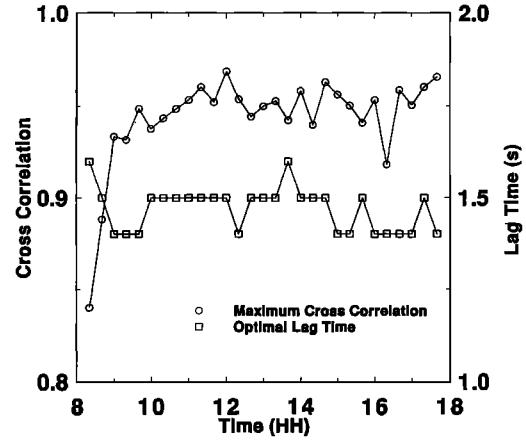

Figure 7a. Correction for LICOR 6262 lag time using a Krypton hygrometer. The optimal lag time resulting in maximum cross correlation is presented. The maximum cross-correlation value between the two water vapor measurements is also shown.

introduces other uncertainties such as the adequate sampling time to obtain a representative mean concentration at each level. In order to evaluate this inadequacy in the profile measurements, a comparison with the 10 Hz LICOR 6262 at 9 m was carried out.

During this experiment the profile-sampling system measured the mean CO_2 concentration at 9 m throughout the day, and we compared these readings to the LICOR 6262 mean concentration measurement (12,000 points) every 20 min. This comparison is shown in Figure 7b. We note that the two air ports are separated by about 2 m. Notice that the profile-measured concentrations are smoother, indicating some loss in the mean concentration value.

Appendix C: Eulerian Integral Timescales via Zero Crossings

Lenschow et al. [1994] found that earlier integral timescale estimates by *Lenschow and Stankov* [1986] may have been overestimated due to the use of the zero-crossing method. They proposed an alternate method which fits an exponential autocorrelation to the measured autocorrelation using regression analysis (they used the Fourier domain instead of the time domain). Using the "best fit" exponential autocorrelation function, the integral timescale can be computed analytically without the need of numerical integration or zero-crossing determination. The reported difference between the two calculations was a factor of 4 for temperature fluctuations. In this appendix we further explore the zero-crossing method in relation to the method of *Lenschow et al.* [1994]. For illustration purposes we computed the autocorrelation function for the vertical velocity time series for a run collected at 0930. The measured autocorrelation function is shown in Figure 8a. The exponential autocorrelation function fit is also shown (dashed line). The integral timescale computed by a trapezoidal integration up to the first zero crossing is 1.5 s, while the integral timescale computed from an analytic integration of the fitted exponential function is 2.0 s. Hence the *Lenschow et al.* [1994] method and the zero-crossing method differ by 25%, which is much smaller than the difference reported by *Lenschow et al.* [1994]. Also, in Figure 8b we show that the method of *Lenschow et al.* [1994] will systematically yield integral timescale values larger than the zero-crossing method due to the unit

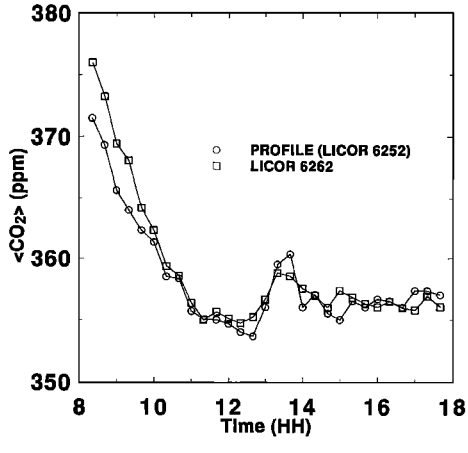

Figure 7b. Comparison between the profile measured CO_2 concentration (LICOR 6252) and the eddy correlation measured CO_2 concentration (LICOR 6262).

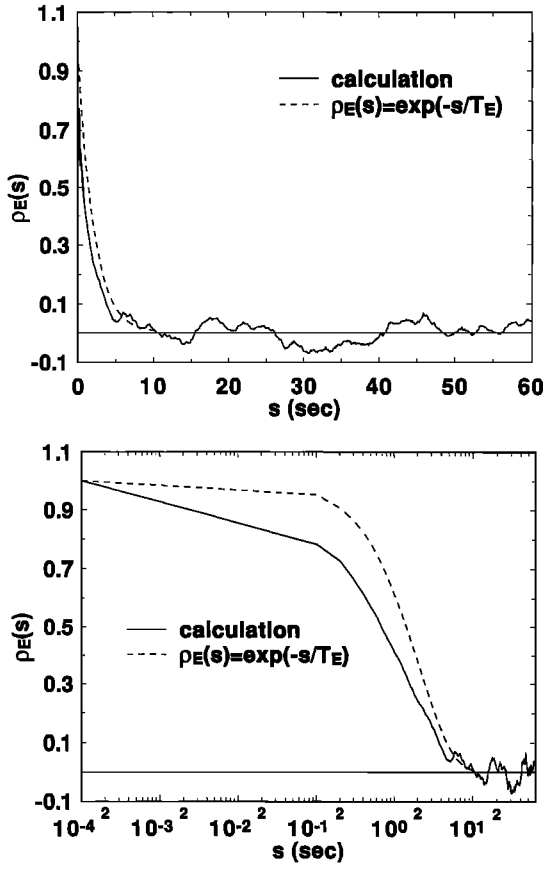

Figure 8. Comparisons between measured (solid) and estimated (dashed) autocorrelation functions shown on (a) a real time lag axis and (b) a log time axis. The estimation was carried out using the method of *Lenschow et al.* [1994].

slope at lag 0 (a logarithmic axis is chosen to amplify the differences at small time lags). We should note that *Lenschow et al.*'s [1994] revised integral timescale values were smaller than the values computed by the zero-crossing method in the work by *Lenschow and Stankov* [1986]. This clearly suggests that the discrepancy could not have been attributed to the zero crossing. Also, note that *Lenschow and Stankov* [1986] used the raw temperature time series, while *Lenschow et al.* [1994] used filtered time series. The temperature time series filtering can remove undesirable trends and low-frequency fluctuations that significantly reduce the decay of the autocorrelation function. Hence the discrepancy in the integral timescale estimates by *Lenschow and Stankov* [1986] and *Lenschow et al.* [1994] is likely due to the filtering scheme. We decided to use the zero-crossing method since the decay of the measured autocorrelation function is finite at finite lags in contrast to the exponential model [also *Lumley and Panofsy*, 1964, pp. 36–37].

Appendix D: Comments on Computation Grid Nodes and Concentration Measurements

It was suggested by *Raupach* [1989a] that dz be chosen such that its magnitude centers vertical concentration measurements. In effect, *Raupach*'s [1989a] approach fragments the canopy into layers with variable thickness dz and assumes that the mean concentration along dz is constant, identical to the measured value. The resultant source profile from such an

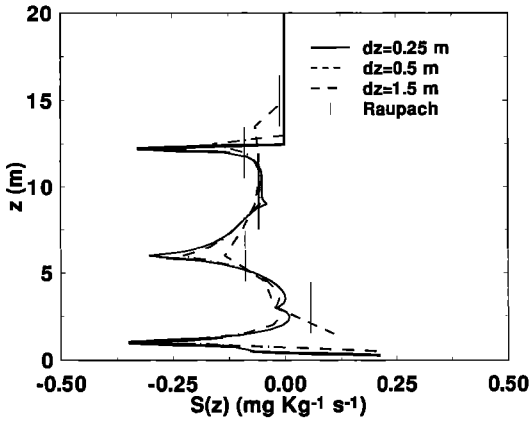

Figure 9a. The influence of dz on the LNF computed source profile for the turbulence measurements in Figure 3d.

assumption is generally discontinuous. In this study we departed from Raupach's suggestions and assumed that the concentration profile is continuous. Hence dz was chosen small enough (relative to the canopy height) to simulate a continuous concentration profile but not so small as to result in a large number of simultaneous equations whose solution is susceptible to numerical instabilities. Furthermore, dz should not be chosen smaller than the Kolmogorov microscale (~1 mm). Hence with this near-continuous concentration profile, the resultant source profile will also be continuous. A key advantage to a near-continuous source profile is in the computation of the flux profile by numerically integrating $S(z)$ with respect to z.

We have repeated the source and flux profile calculations for all runs using dz = 0.1, 0.25, 0.5, 1.5, and 3.0 m in order to assess the effects of discretization on the computed fluxes at z = 9 m. These dz values were chosen such that the computed and measured CO_2 flux nodes at z = 9 m coincide. Also, the last dz (3 m) roughly coincides with Raupach's suggestions.

As an illustration the computed source and flux profiles for the run in Figure 3d are reproduced in Figures 9a and 9b for dz = 0.25, 0.5, 1.5, and 3 m. For dz = 0.1 m, the resultant source and flux profiles were identical to those obtained with dz = 0.25 m and are not shown for clarity purposes. While the same qualitative features are evident in all source profile calculations (Figure 9a), the flux profiles are very different (Figure 9b). Since the computed flux at z = 9 m using Raupach's

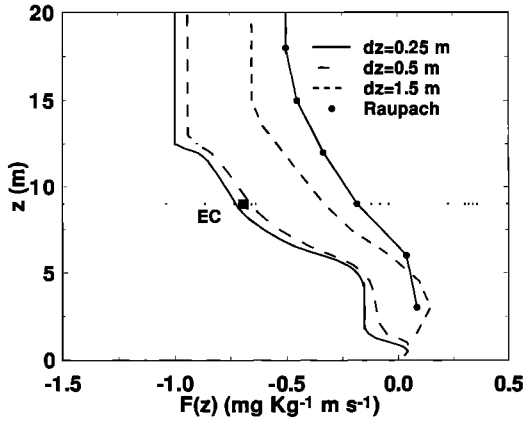

Figure 9b. Same as Figure 9a, but for the flux profile. The eddy correlation measured flux is also shown.

Table 1. Influence of dz on the Comparison Between Predicted and Measured CO_2 Flux at z = 9 m for All Runs

dz, m	Slope A	Intercept B	r^2	SEE
0.10	0.981	−0.0431	0.57	0.16
0.25	0.978	−0.0533	0.58	0.16
0.50	0.840	−0.103	0.52	0.16
3.00	0.794	0.330	0.43	0.18

The regression model is $F_c = AF_c^{(ec)} + B$. The standard error of estimate (SEE) and the coefficient of determination (r^2) are also shown.

method differs by a factor of 2 from the eddy correlation value for this run, we decided to recompute and summarize the comparison between predicted and measured fluxes at z = 9 m for all runs in Table 1 using dz = 0.1, 0.25, 0.5, and 3.0 m, respectively. Notice that for dz = 0.1, 0.25, and 0.5 the regression statistics are very comparable and superior to the results obtained with dz = 3.0 m. Based on these results, the proposed approach may be more adequate than a discontinuous source profile.

Acknowledgments. The authors would like to thank George Hendrey and John Sigmon for their support, Greg Kuhn and Judd Edburn for their assistance at the Duke Forest, Bart Van den Hurk for his helpful comments and suggestions, and one of the anonymous referees for pointing out the study by Dolman and Wallace. This project was funded, in part, by the Environmental Protection Agency (EPA) under cooperative agreement 91-0074-94 (CR817766), the National Science Foundation (NSF-BIR12333), and the U.S. Department of Energy (DOE) through the National Institute for Global Environmental Change (NIGEC) through the Southeast Regional Center at the University of Alabama, Tuscaloosa (DOE cooperative agreement DE-FC03-90ER61010) and the Office of Health and Environmental Research (DE-ACO2-76CH00016).

References

Angell, J. K., Lagrangian-Eulerian time-scale relationship estimated from constant volume balloon flights past a tall tower, *Adv. Geophys., 18A*, 419–431, 1974.

Baldocchi, D., A Lagrangian random walk model for simulating water vapor, CO_2 and sensible heat flux densities and scalar profiles over and within a soybean canopy, *Boundary Layer Meteorol., 61*, 113–144, 1992.

Batchelor, G. K., *The Theory of Homogeneous Turbulence*, 197 pp., Cambridge Univ. Press, New York, 1953.

Corrsin, S., Progress report on some turbulent diffusion research, *Adv. Geophys., 6*, 161–164, 1959.

Corrsin, S., Estimates of the relations between Eulerian and Lagrangian scales in large Reynolds number turbulence, *J. Atmos. Sci., 20*, 115–119, 1963.

Corrsin, S., Limitations of gradient transport models in random walks and in turbulence, *Adv. Geophys., 18A*, 25–60, 1974.

Csanady, G. T., *Turbulent Diffusion in the Environment*, 250 pp., D. Reidel, Norwell, Mass., 1973.

Deardorff, J. W., Closure of second- and third moment rate equations for diffusion in homogeneous turbulence, *Phys. Fluids, 21*, 525–530, 1978.

Denmead, O. T., and E. F. Bradley, Flux-gradient relationships in a forest canopy, in *The Forest-Atmosphere Interaction*, edited by B. A. Hutchison and B. B. Hicks, pp. 421–442, D. Reidel, Norwell, Mass., 1985.

Dolman, A. J., and J. S. Wallace, Lagrangian and K-theory approaches in modeling evaporation from sparse canopies, *Q. J. R. Meteorol. Soc., 117*, 1325–1340, 1991.

Du, S., J. D. Wilson, and E. Yee, On the moments approximation method for constructing a Lagrangian stochastic model, *Boundary Layer Meteorol., 70*, 273–292, 1994.

Dyer, A. J., and B. B. Hicks, Flux-gradient relationships in the constant flux layer, *Q. J. R. Meteorol. Soc.*, *96*, 715–721, 1970.

Ellsworth, D. S., R. Oren, C. Huang, N. Phillips, and G. R. Hendrey, Leaf and canopy responses to elevated CO_2 in a pine forest under free-air CO_2 enrichment, *Oecologia*, *104*, 139–146, 1995.

Finnigan, J. J., and M. R. Raupach, Transfer processes in plant canopies in relation to stomatal characteristics, in *Stomatal Function*, edited by E. Zeiger, G. D. Farquhar, and I. R. Cowan, pp. 385–429, Stanford Univ. Press, Stanford, Calif., 1987.

Fischer, H. B., E. List, R. Koh, J. Imberger, and N. Brooks, *Mixing in Inland and Coastal Waters*, 483 pp., Academic, San Diego, Calif., 1979.

Gardiner, C. W., *Handbook of Stochastic Methods for Physics, Chemistry, and the Natural Sciences*, 442 pp., Springer-Verlag, New York, 1990.

Horst, T. W., and J. C. Weil, Footprint estimation for scalar flux measurements in the atmospheric surface layer, *Boundary Layer Meteorol.*, *59*, 279–296, 1992.

Hunt, J. C. R., Diffusion in the stable boundary layer, in *Atmospheric Turbulence and Air Pollution Modelling*, edited by F. T. M. Nieuwstadt and H. van Dop, pp. 231–274, D. Reidel, Norwell, Mass., 1982.

Kaimal, J. C., and J. J. Finnigan, *Atmospheric Boundary Layer Flows: Their Structure and Measurement*, 289 pp., Oxford Univ. Press, New York, 1994.

Katul, G. G., A model for sensible heat flux probability density function for near-neutral and slightly stable atmospheric flows, *Boundary Layer Meteorol.*, *71*, 1–20, 1994.

Katul, G. G., M. B. Parlange, J. D. Albertson, and C. R. Chu, Local isotropy and anisotropy in the sheared and heated atmospheric surface layer, *Boundary Layer Meteorol.*, *72*, 123–148, 1995.

Leclerc, M. Y., and G. W. Thurtell, Footprint prediction of scalar fluxes using a Markovian analysis, *Boundary Layer Meteorol.*, *52*, 247–258, 1990.

Leclerc, M. Y., G. W. Thurtell, and G. E. Kidd, Measurements and Langevin simulations of mean tracer concentration fields downwind from a circular line source inside an alfalfa canopy, *Boundary Layer Meteorol.*, *43*, 287–308, 1988.

Legg, B. J., and M. R. Raupach, Markov-chain simulation of particle dispersion in inhomogeneous flows: The mean drift velocity induced gradient in Eulerian velocity variance, *Boundary Layer Meteorol.*, *24*, 3–13, 1982.

Lenschow, D. H., and B. B. Stankov, Length scales in the convective boundary layer, *J. Atmos. Sci.*, *43*, 1198–1209, 1986.

Lenschow, D. H., J. Mann, and L. Kristensen, How long is long enough when measuring fluxes and other turbulence statistics?, *J. Atmos. Ocean. Technol.*, *11*, 661–673, 1994.

Ley, A. J., and D. J. Thomson, A random walk model of dispersion in the diabatic surface layer, *Q. J. R. Meteorol. Soc.*, *109*, 847–880, 1983.

Luhar, A., and R. Britter, A random walk model for dispersion in inhomogeneous turbulence in a convective boundary layer, *Atmos. Environ.*, *23*, 1911–1924, 1989.

Lumley, J., and H. A. Panofsky, *The Structure of Atmospheric Turbulence*, 239 pp., John Wiley, New York, 1964.

McComb, W. D., *The Physics of Fluid Turbulence*, 571 pp., Oxford Univ. Press, New York, 1990.

McNaughton, K. G., and B. J. J. M. Van den Hurk, A Lagrangian revision of the resistors in the two-layer model for calculating the energy budget of a plant canopy, *Boundary Layer Meteorol.*, *74*, 261–288, 1995.

Meyers, T., and D. D. Baldocchi, A comparison of models for deriving dry deposition fluxes of O_3 and SO_2 to a forest canopy, *Tellus*, *40B*, 270–284, 1988.

Meyers, T. P., and K. T. Paw U, Testing of a higher-order closure model for modeling air flow within and above plant canopies, *Boundary Layer Meteorol.*, *37*, 297–311, 1986.

Meyers, T. P., and K. T. Paw U, Modeling the plant-canopy micrometeorology with higher-order closure principles, *Agric. For. Meteorol.*, *41*, 143–163, 1987.

Monin, A. S., and A. M. Yaglom, *Statistical Fluid Mechanics*, 769 pp., MIT Press, Cambridge, Mass., 1971.

Pasquill, F., and F. B. Smith, *Atmospheric Diffusion*, 437 pp., John Wiley, New York, 1983.

Press, W. H., S. A. Teukolsky, W. T. Vetterling, and B. P. Flannery, *Numerical Recipes*, 963 pp., Cambridge Univ. Press, New York, 1992.

Raupach, M. R., Near-field dispersion from instantaneous sources in the surface layer, *Boundary Layer Meteorol.*, *27*, 105–113, 1983.

Raupach, M. R., Canopy transport processes, in *Flow and Transport in the Natural Environment*, edited by W. L. Steffen and O. T. Denmead, pp. 95–127, Springer-Verlag, New York, 1988.

Raupach, M. R., Applying Lagrangian fluid mechanics to infer scalar source distributions from concentration profiles in plant canopies, *Agric. For. Meteorol.*, *47*, 85–108, 1989a.

Raupach, M. R., A practical Lagrangian method for relating scalar concentrations to source distributions in vegetation canopies, *Q. J. R. Meteorol. Soc.*, *115*, 609–632, 1989b.

Raupach, M. R., O. T. Denmead, and F. X. Dunin, Challanges in linking atmospheric CO_2 concentrations to fluxes at local and regional scales, *Aust. J. Bot.*, *40*, 697–716, 1992.

Reid, J. D., Markov chain simulations of vertical dispersion in the neutral surface layer for surface and elevated releases, *Boundary Layer Meteorol.*, *16*, 3–22, 1979.

Sawford, B. L., Lagrangian statistical simulation of concentration mean and fluctuating fields, *J. Clim. Appl. Meteorol.*, *24*, 1152–1166, 1985.

Sawford, B. L., Generalized random forcing in random-walk turbulent dispersion models, *Phys. Fluids*, *29*, 3582–3585, 1986.

Sawford, B. L., Recent developments in the Lagrangian stochastic theory of turbulent dispersion, *Boundary Layer Meteorol.*, *62*, 197–215, 1993.

Snyder, W. H., and J. L. Lumley, Some measurements of particle velocity autocorrelation functions in a turbulent flow, *J. Fluid Mech.*, *48*, 41–71, 1971.

Taylor, G. I., Diffusion by continuous movements, *Proc. London Math Soc., Ser. A*, *20*, 196–211, 1921.

Tennekes, H., and J. L. Lumley, *A First Course in Turbulence*, 300 pp., MIT Press, Cambridge, Mass., 1972.

Thomson, D. J., Criteria for the selection of stochastic models of particle trajectories in turbulent flows, *J. Fluid Mech.*, *180*, 529–556, 1987.

Thurtell, G. W., Comments on using K theory within and above plant canopy to model diffusion processes, in *Estimation of Areal Evapotranspiration*, edited by T. A. Black, D. L. Spittlehouse, M. D. Novak, and D. T. Price, *IAHS Publ.*, *177*, pp. 81–85, 1989.

Van den Hurk, B. J. J. M., and K. G. McNaughton, Implementation of near-field dispersion in a simple two-layer surface resistance model, *J. Hydrol.*, *166*, 293–311, 1995.

Wilson, J. D., Turbulent transport within plant canopy, in *Estimation of Areal Evapotranspiration*, edited by T. A. Black, D. L. Spittlehouse, M. D. Novak, and D. T. Price, *IAHS Publ.*, *177*, pp. 43–80, 1989.

Wilson, J. D., and T. K. Flesch, Flow boundaries in random-flight dispersion models: Enforcing the well-mixed conditions, *J. Appl. Meteorol.*, *32*, 1695–1707, 1993.

Wilson, J. D., G. W. Thurtell, and G. E. Kidd, Numerical simulation of particle trajectories in inhomogeneous turbulence, I, Systems with constant turbulent velocity scales, *Boundary Layer Meteorol.*, *21*, 295–313, 1981a.

Wilson, J. D., G. W. Thurtell, and G. E. Kidd, Numerical simulation of particle trajectories in inhomogeneous turbulence, II, Systems with variable turbulent velocity scales, *Boundary Layer Meteorol.*, *21*, 423–441, 1981b.

Wilson, J. D., B. J. Legg, and D. J. Thomson, Calculation of particle trajectories in the presence of a gradient in turbulent-velocity variance, *Boundary Layer Meteorol.*, *27*, 163–169, 1983.

Wofsy, S. C., M. L. Goulden, J. W. Munger, S. M. Fan, P. S. Bakwin, B. C. Daube, S. L. Bassow, and F. A. Bazzaz, Net exchange of CO_2 in a mid-latitude forest, *Science*, *260*, 1314–1317, 1993.

D. Ellsworth and K. Lewin, Department of Applied Sciences, Brookhaven National Laboratory, Upton, NY 11973-5000. (e-mail: ellswort@bnl.gov; lewin@bnl.gov)

C.-I. Hsieh, G. Katul, R. Oren, and N. Phillips, School of the Environment, Duke University, Durham, NC 27708. (e-mail: hsieh@acpub.duke.edu; gaby@acpub.duke.edu; Ramoren@duke.edu; nphillip@acpub.duke.edu)

(Received May 18, 1995; revised October 14, 1996;
accepted December 9, 1996.)